Solids Fractions and Flow Characteristics in a CFB as Measured with a Fiber Optic Probe

Steven M. Seachman, Paul C. Yue, Emily M. Taylor, and Lawrence J. Shadle
U.S. DOE National Energy Technology Laboratory
Morgantown, WV 26507-0880

Abstract

A multi-fiber optical reflective probe was used to measure particle velocities and solids loading in the riser of a 0.3 m circulating fluidized bed (CFB). Using statistically designed tests the probe was inserted at radial positions, varying heights, and azimuthal locations over two solids flux conditions for a single riser gas velocity. An equation to was developed to calculate the localized solids fraction based on the Beer-Lambert Law. These solid fractions were compared with those estimated from pressure drop measurements and literature. The values followed the trend of the pressure measurements and previous calculations. In addition, the measurements found with the probe also illustrated that the solids fraction in the riser was more dilute in the center of the riser and became dense as it approached the wall. While the mean particle velocities were symmetric around different azimuthal positions in the riser their fluctuations were not. These fluctuations were characterized using the turbulent kinetic energy analysis. Solids fraction in the fully developed region of the riser was relatively symmetric. In addition, the concentration and distribution did not change after entering the fully developed region. Because the fiber optic probe only picks up a portion of the reflected light, further calibration of the probe will be needed to obtain exact values of the solids fraction.

Introduction

For many years, circulating fluidized beds have been studied using a vast array of instrumentation to improve upon numerous industrial applications such as coal power plants and metallurgy processes. Reflective optical fiber probes have been used as one of the many tools to collect data from CFB testing **[1-10]**. Two of the most common uses of the probe are to measure local bed voidage and particle velocities.

There are many advantages to using reflective optical fiber probes in Fluidized Bed applications. Most probes are inexpensive being fabricated using stainless steel tubing, making the probe reasonably durable. The diameters of these probes are also typically small, causing fewer disturbances in the flow of the system and traverse across the entire diameter of the riser. Fiber optic probes' signals are not affected by humidity or temperature.

Reflective optical fiber probes vary in numerous characteristics. One of the ways that they vary is in the amount of fibers used. Some use two large fibers, one for receiving and one for transmitting **[1, 3-6, 9],** to obtain the needed measurements while others use many small fibers to transmit and receive light **[2, 7, 8, 10]**. A number of fiber-optic probes use lasers as their source of light **[3, 5, 6]** while others use unfocused

light such as LEDs **[1, 2, 4, 7-10]**. Several probes use a defined sampling volume **[1, 3, 4, 9]** while others direct the light straight out from the bundles **[2, 4-10]**.

Even though the velocity measurements found with these probes are typically straight forward, there are some problems involved with using reflective optical fiber probes to measure voidage. The techniques implemented to calculate voidage from the measurements typically use a straight-line relationship. This is an inaccurate method of calculating voidage due to the fact that the reflected light is not a linear function of particle loading. Also, a large or undefined sampling volume can create problems interpreting the results. Studies have also shown that the calibration of the probe for use in voidage measurements is material dependent **[1, 3-5, 9, 10]** due to differences in reflective properties and particle diameter shown in.

In this study, a reflective optical multi-fiber probe was used to measure localized solids fraction and velocity within the riser of a circulating fluidized bed operated in a densely solids loaded, core-annular flow regime. The local solids fractions were found using the reflected light from the particle measured with the probe analyzed using an equation derived from the Beer-Lambert law. These values were then compared to literature and solids fractions found with pressure drop measurements. The utility of this technique to evaluate mixing was demonstrated by testing for symmetry across the riser. The fractions and velocities were taken at different azimuthal locations around the circumference of the riser at different axial locations and mass circulation rates (M_s). The resulting data was evaluated statistically to check for validity of the measurements.

Experimental Facility

The cold flow, circulating fluidized bed (CFB) was tested at the National Energy Technology Laboratory in Morgantown, West Virginia. The dimensions and layout are shown in Figure 1. Solid glass spheres with an average diameter of 64 □m were the test bed material. The tests conducted included varying independently the solids circulation rate and sampling location including the axial, radial, and azimuthal positions, while the gas density and superficial velocity were kept constant. This represents a full factorial design. The

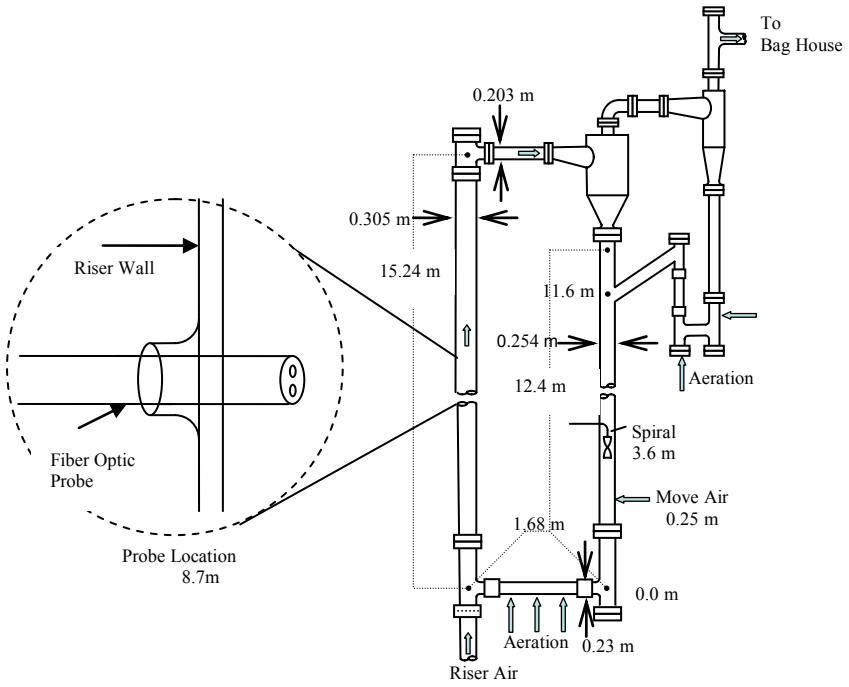

Figure 1 – CFB setup and probe location

dependent measurements included optical fiber readings as well as process information – most notably the incremental pressure drops. The CFB was run at two different conditions. The superficial gas velocity (U_g) was fixed at 5.17 m/s and the M_s values at 5,400 kg/hr for the dilute flow condition and 33,500 kg/hr for the core annular flow condition were used. Both conditions were in the transport flow regime above the second transport velocity as defined by Monazam et al. **[11]**.

The probe used was a multi-fiber reflective optical probe developed by Vector Scientific Instruments. The probe contains two 1 millimeter diameter bundles each with 300 minute optical glass fibers. There are equal amounts of randomly distributed transmitting and receiving fibers within each bundle. Light is transmitted through the fibers from a light emitting diode (LED) and the reflected light from the particles is then received by the instrument via photocell. The signal from the photocell is transferred into the computer through an A/D Converter. For each run, 1024 measurements were taken for each of 200 sample periods at a rate of 12.5 kHz over a period of approximately 30 s. The signals from each of the fiber optic bundles were then cross-correlated to determine the particle transit times in each 30 ms sampling periods. The velocities were calculated knowing the translational distance between the fibers. The particle velocity was verified using a steel fiber rotated in front of the probe at fixed rates as determined by a stroboscopic sensor. The sampling rate was selected to optimize the probe accuracy over the expected particle velocity range. Particle turbulent kinetic energy (TKE), which is the velocity fluctuation from the mean, was determined by taking the root mean square of the velocities. The solids voidage was determined from the amplitude of the reflected light signal as described in the theoretical section below.

The optical probe was placed 8.7 meters above the centerline of the solids recycle inlet at the bottom of the riser. The location was considered in the fully developed flow based upon the axial pressure profile. At each location the probe was traversed through the mid points of five equal areas inside the riser. These points were taken in a randomized order as were the operating conditions. The probe was also placed in three different and randomized azimuthal locations (0, 90, and 270 degrees). However, the azimuthal variable was blocked, which means that the five radial positions were taken at one location, then moved to another azimuthal location. In order for this test to be totally random, each radial position as well as azimuthal location should have been taken individually. Further discussion of this can be found in the results and discussion section.

Theory

The basis behind the voidage calculation is that light is transmitted, reflected, or absorbed when passing through a medium. Hence,

$$I_0 = I_T + I_{ext} + I_A \quad (1)$$

Since glass beads were used it was assumed that the absorption of light (I_A) was negligible. This assumption was also used by Hoffman when developing Christiansen Filters **[12]**. In practice, this assumption may not be appropriate in an industrial scale facility such as the one used here; however, the trends are expected to still be valid.

The light intensities (I) are then normalized with respect to the total light emitted from the probe;

$$1 = R + T \tag{2}$$

where,

$$R = \frac{I_R}{I_0} \quad \text{and} \quad T = \frac{I_T}{I_0} \tag{3}$$

The above equations were then rearranged to solve for transmission of light in the system. $I_T = I_0 - I_R$ (4)

or

$$T = 1 - R \tag{5}$$

The Beer-Lambert law for light transmission through a medium of particles can be written in the following form:

$$T = e^{-c(1-\varepsilon)L} \tag{6}$$

where c is the extinction coefficient, (1-□) is the solids fraction and L is the path length. Since c does not vary with length or concentration, it is considered constant. Additionally, since an LED is used as the light source, the path length is very small, and also considered constant. Therefore, solids fraction is the only value that changes with transmission. Miller et al. (1992) used the Beer-Lambert law to calculate solids fraction using radiation and transmission **[13]**. The natural log of both sides is taken in order to solve for solids concentration.

$$\ln(T) = K(1-\varepsilon) \tag{7}$$

The values of total light intensity and reflected light intensity are substituted from equation (5) to yield the equation used to find the localized solids fraction.

$$\ln(1-R) = -K(1-\varepsilon) \tag{8}$$

When plotted, Equation 8 is linear on a log-linear graph. Hence the equation takes the form y=mx+b, where y is the left hand side, K is the slope, the solids fraction (1-□) is x, and b is the signal recorded by the fiber optic probe, which will be discussed further in the calibration section.

Calibration

Four values are needed in order to calibrate the fiber optic probe for solids fraction measurements. The first one is the total light intensity that the probe emits, I_0. This was found by taking a series of measurements with a mirror placed directly in front of the probe. Two values were determined by the probe for each bundle of fibers. The next values needed are the intensities of light reflected, I_R, from glass beads at known solids concentrations; a packed bed and when no beads were present were the two known values used. The values taken in an empty riser were recorded in order to account for the noise that the probe encounters. These values were then used as the known values to solve for K. Both I_0 and K were assumed constant.

Table 1 contains the values for the calibration curves for both sets of bundles. The two bundles have different calibration curves due because the input and output of light vary between both bundles. The value b is included in the equation to correct for the fact that the optical fiber probe does not read zero in an empty bed. The value is very low and acts as a zero for the calibration.

Table 1 *– Calibration values for fiber optic probe*

	Bundle 1	Bundle 2
I_o	4.6209	3.4221
$I_{r\ packed}$	1.0706	0.8576
$I_{r\ empty}$	0.0141	0.0203
K	0.4441	0.4817
b	-0.0031	-0.0059

In order to characterize the beam divergence, the probe was once again placed in a packed bed of glass beads, and then backed out of the bed in one-millimeter increments. Figure 2 depicts the data from this procedure. From the data plotted in Figure 2 it can seen that the reflected light intensity drops off rapidly if the sampling volume is not within 2 mm of the probe surface.

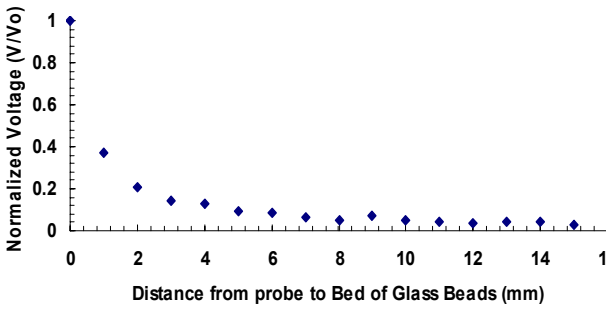

Figure 2 – Normalized Light Intensity as a function of distance from packed bed of glass spheres

After this test was performed, the solids fractions found with the fiber optic probe were compared against the apparent solids holdup **[1]**. This is found from the change in pressure between two axial locations divided by the length in between the taps and assuming that the pressure drop was due to the weight of the bed thereby ignoring the relatively small contributions from gas-wall and solids friction. This value is then divided by the density of the bed material.

$$(1-\varepsilon)=\left[\frac{(144*\Delta P)}{\Delta L}\right]\Big/\rho_{glass} \qquad (9)$$

Table 2 *- Solids concentration comparison*

Load Ratio	$(1-\varepsilon)_{optic}$	$(1-\varepsilon)_{pressure}$
3.27	**0.024**	**0.005**
19.65	**0.076**	**0.036**

The solids concentration measured from pressure drop and optical probe methods are displayed in Table 2. These were taken at the upper riser location (8.7 m above the riser inlet) in a region where the flow was fully developed. Because the pressure drop represents an average solids fraction while the optical method is local, the optical method was integrated across the cross section to compare the values. This was done by taking 5 samples across the radius at points representing equal area regions of the riser. The optical measurements were also tested by comparing the integrated product of the particle velocity and concentration against the average solids flux. The integrated fluxes were found to be a factor of 2 to 3 higher. Even though the average values did not correspond, they followed the same trend, namely, as the values calculated from pressure drop increased, the values calculated from the fiber optic probe also increased. Likewise for the solids fluxes, the integrated solids fluxes increased as the controlled solids fluxes were increased. There are at least two possible explanations for these discrepancies: the solids-gas frictional contributions may not have been insignificant, and light absorption by the bed may not be negligible.

The trends found with the fiber optic probe calibration were compared against literature that also used a fiber optic probe with different calibration for solids fraction calculations **[10]**. Figure 3 illustrates the comparison between the two different methods of calibration. The curve is the data found using the Beer-Lambert law theory, and solving for the intensity, I_R, where the points represent data found from Zhang et al. The K value differed from the value used in this study due to the fact that K is material dependent. The material used in Zhang was FCC catalyst, where the study discussed here was glass spheres.

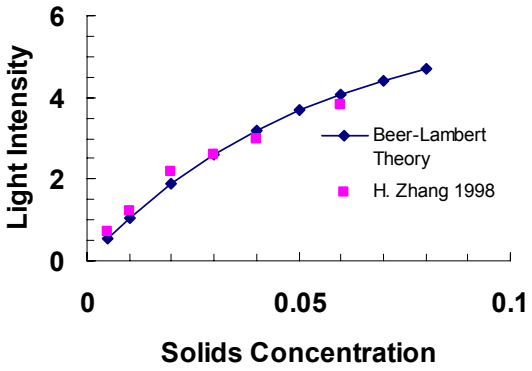

Figure 3 – Comparison of Solids Concentration Calculation Methods

Results and Discussion

Figures 4 and 5 illustrate the mean velocities, solids fractions, and particle turbulent kinetic energy for the two conditions tested. The velocity profiles were higher towards the center of the riser and decreased closer to the wall. Inversely, both solids fraction profiles were dilute in the center and increased in solids fraction as it approached the wall.

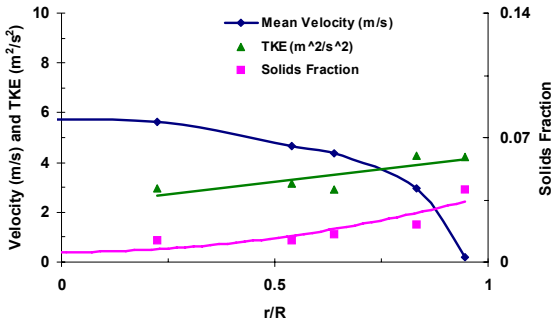

Figure 4 – CFB Dynamics for Load Ratio of 3.2

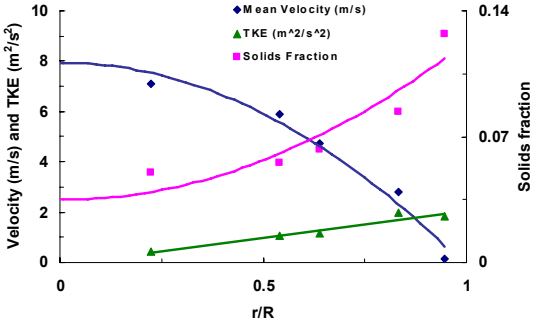

Figure 5 – CFB Dynamics for Load Ratio of 19.8

The TKE was generally higher for the lower solids flux condition. The particle velocity profile for the lower flux case was a typical single phase turbulent velocity profile. The low solids flux does not compromise the fluid flow patterns and as a result the values of TKE are a factor of 2 to 4 times higher than the higher solids flux condition. In the higher solids flux condition the particle compromise the flow profiles creating a typical parabolic particle velocity profile. This can be interpreted as a result of the dampening of particle velocity fluctuations in clusters where velocity fluctuations have been reported to be much lower than in the dispersed phase [14]. On the average the particle TKE increased linearly as it approached the wall. The particle turbulence was somewhat stable in the higher velocity central core but turbulence

increased nearer the wall in the higher solids annular region of the riser. The variability in the particle turbulence kinetic energy data was higher in this annular region near the wall.

To check for azimuthal dependency in the fully developed region as well as test for which factors significantly contribute to the variability of each dependent parameter total average velocity (TAV), solids fraction, and TKE, several analysis of variance (ANOVA) were performed. Because the average was taken from large amounts of data, from the central limit theorem, the data is approximately normally distributed. This validates the results of the ANOVA. Significance was determined at the 95% confidence level. The results can be found in Table 3. For ANOVA conducted on the TAV the only main effect to have a significant impact was radial position, r/R. In addition, there was an existence of second order curvature within r/R as indicated by probabilities (p-values) less than 0.05.

It is interesting to note that the solids velocity was not significantly dependent on the solids circulation rate. This suggests that even though there was a large difference in the overall pressure drops in the riser both were in a similar core annular structure. However, a p-value of 0.0139 indicated a significant interaction between r/R and M_s. This implies a different trend in the radial profiles for varying M_s. The particle velocities dropped off from the peak in the center beyond a radial position of 0.54 at the high M_s, but it did not begin to drop off until a radial position of 0.83 for the lower M_s. The amount of variability explained by these variables was approximately 91%.

For solids fraction, the only effects that did not significantly contribute to its variability were the azimuthal position terms, degree and degree^2. Increasing Ms from low to high load ratio caused a significant increase in solids fraction. The solids fraction was significantly higher nearer the wall and this dependence on radial position was non-linear as indicated by the statistically significant r/R^2 term. On the contrary, the solids fraction was not significantly affected by azimuthal position.

For particle turbulent kinetic energy, all three main effects significantly affect the response, while the azimuthal location also displayed significant second-order curvature. This model explained about 56% of the variability that was seen within the turbulent kinetic energy, suggesting there was an unmeasured variable that should have been included in the model.

It is also desired to test for an interaction between degree and r/R. However, in the order of test runs, the variable degree was not randomized, so this interaction can not be

formally tested. It can be approximated in spite of this by examining Figure 6 in which the values for solids velocity are averaged for different levels of M_s. An interaction is demonstrated: at different r/R positions the value of degree that will produce the largest and smallest TAV is not constant. It is interesting to note that at the fourth r/R position, 0.83, all values are approximately equal.

The non-formal check for an interaction between degree and r/R for solids concentration can be evaluated by inspecting Figure 7. Again the values of solids fraction were averaged over both circulation rates, M_s. There appears to be only a slight interaction between degree and r/R as it only can be seen at the last two positions near the wall. This implies that the annular region was confined to the outer two radial positions beyond r/R of 0.83.

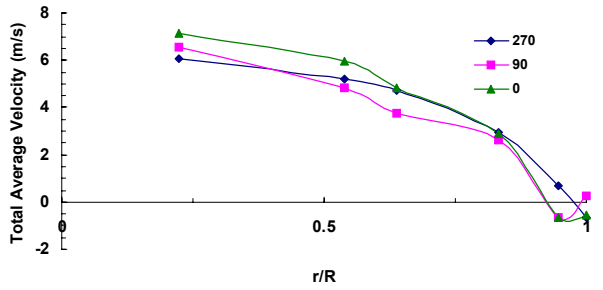

Figure 6 – Interaction of Total Average Velocity

For the TKE response, again the interactions containing degree cannot be formally tested because of the run order. However, the data displayed in Figure 8 indicates that there was a significant interaction between r/R and degree because TKE taken at 0 degree peaked near the transition between core and annulus, while those taken 90 degrees off the inlet plane trended higher towards the wall. This was observed in both the low and high flux data sets. It is unclear why the asymmetry in riser inlet and outlet configurations was exhibited in only this parameter at this midpoint elevation.

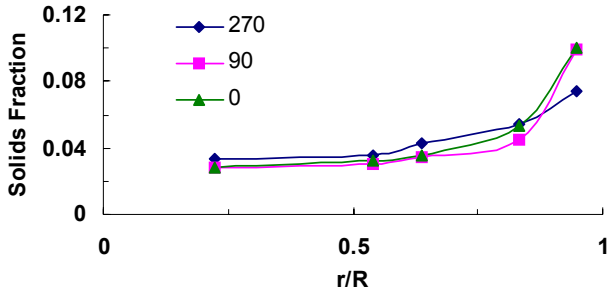

Figure 7 – Solids Concentration Interaction

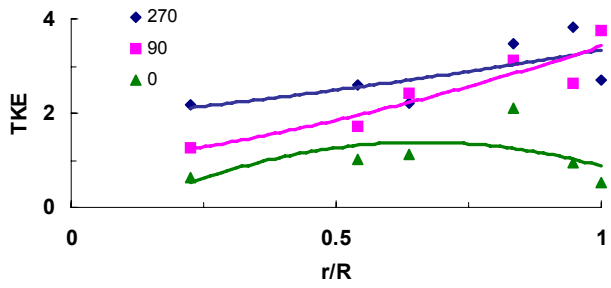

Figure 8 – Turbulent Kinetic Energy Concentration Interaction

Summary

The calibration was sufficient to measure the trend of the solids fraction profiles within the riser. However, further calibration is needed in order to obtain exact values of solids loading in the riser. It is known that the fiber optic probe only receives portions of the total reflected light, which is an important factor in using the Beer-Lambert Law to solve for solids loading. Moreover, probes do not have to be removed and moved to a different position during testing, which decreases down time and time in order to complete a test run

According to the statistical analyses performed on the data in the fully developed region, there were no azimuthal dependencies with regard to total average velocities and solids fraction. This means that measurements can be taken for one half of the bed instead of having to traverse though the entire diameter.

Even though the TKE evaluation is not complete, it is a valuable tool in studying the particle behavior inside of the CFB riser. TKE is an excellent parameter in studying the impact that the inlet and outlet have on the entirety of the riser.

Acknowledgements

The authors would like to acknowledge contributions from Ronald Breault, J. Christopher Ludlow, and James Spenik for their part in operations, measurements, and analysis. Funding for this project was provided by National Energy Technology Laboratory's Advanced Research program within the Strategic Center for Coal. Steven Seachman's research assistantship was made available through the Oak Ridge Institute for Science Education (ORISE).

References:

1. A. Magnusson, R. Rundqvist, A.E. Almsedt, F. Johnsson. (2005). Dual fiber optical probe measurements of solids volume fraction in a circulating fluidized bed, Powder Technology, 151, 19-26.
2. A. Yan, H. Zhu, J. Zhu. (2004). Comparison of FCC Particle Flow in a Twin-Riser System. ECI Fluidization, 11.
3. H. Johnsson, F. Johnsson. (2001). Measurements of local solids volume-fraction in fluidized bed boilers. Powder Technology, 115, 13-26.
4. L. Reh, J. Li. (1991). Measurement of Voidage in Fluidized Beds by Optical Probes. Circulating Fluidized Bed Technology, 3, 163-170.
5. D. Lischer, M. Louge. (1992). Optical fiber measurements of particle concentration in dense suspensions: calibration and simulation. Applied Optics, 31 (24), 5106-5113.
6. N. Samuel, Krol Stefan, L. Hugo. (2004). Particle Velocity and Particle Clustering in Downflow Reactors: Measurements Using a CREC-GS-Optiprobe. . (2004). Comparison of FCC Particle Flow in a Twin-Riser System. ECI Fluidization, 11.
7. J. Zhou, J. Grace, C. Lim, C. Brereton. (1995). Particle Velocity Profiles in a Circulating Fluidized Bed Riser of Square Cross-Section. Chemical Engineering Sciences, 50 (2), 237-244.
8. J. Zhu, G. Li, S. Qin, F. Li, H. Zhang, Y. Yang. (2001). Direct measurements of particle velocities in gas-solids suspension flow using a novel five-fiber optical probe. Powder Technology, 115, 184-192.
9. R. Rundqvist, A. Magnusson, G. van Wachem, A. Almstedt. (2003). Dual fibre measurements of the particle concentration in gas/solid flows. Experiments in Fluids, 35, 572-579.
10. H. Zhang, P. Johnston, J. Zhu, H. de Lasa, M. Bergougnou. (1998). A novel calibration procedure for a fiber optic solids concentration probe. Powder Technology, 100, 260-272.

11. E.R. Monazam, L.J. Shadle J. Mei, J. Spenik,(2005) Identification and Characteristics of Different Flow Regimes in a Circulating Fluidized Bed, *Powder Technology, 155(1), 17-25.*
12. H-J. Hoffman, (2000), Theory for the Spectral Transmittance of Christiansen Filters made of Glass Beads. Applied Physics, B 70, 853-861.
13. A. Miller, D. Gidaspow. (1992). Dense, Vertical Gas-Solid Flow in a Pipe. AIChE, 38(11), 1801-1815.
14. R.W. Breault, J.C. Ludlow, and P.C. Yue (2005), Cluster Particle Number and Granular Temperature for Cork Particles at the Wall in the Riser of a CFB, Powder Technology, 149 (2-3) pp.68-77